Available online at www.sciencedirect.com
SCIENCE DIRECT
Journal of Molecular Catalysis A: Chemical 246 (2006) 43–48
JOURNAL OF MOLECULAR CATALYSIS A: CHEMICAL
www.elsevier.com/locate/molcata

Effect of promoters in the methane reforming with carbon dioxide to synthesis gas over Ni/HY catalysts

Heondo Jeong [a,b], Kweon Ill Kim [b], Dongsik Kim [b], In Kyu Song [a,*]

[a] *School of Chemical and Biological Engineering, Research Center for Energy Conversion and Storage, Seoul National University, Shinlim-dong, Kwanak-ku, Seoul 151-744, South Korea*
[b] *Hydrogen Separation & Storage Research Center, Korea Institute of Energy Research, Jang-dong, Yuseong-ku, Daejeon 305-343, South Korea*

Received 2 August 2005; received in revised form 13 October 2005; accepted 13 October 2005
Available online 22 November 2005

Abstract

Methane reforming with carbon dioxide to synthesis gas was investigated over a series of Ni/HY catalysts promoted by Mg, Mn, K, and Ca. These catalysts were characterized by XRD, BET, FT-IR, and TGA analyses before and after the reaction. It was observed that Ni-Mg/HY catalyst showed the highest carbon resistance and the most stable catalytic performance. It was also revealed that the addition of Mg promoter reduced the size of nickel species and produced the highly dispersed nickel species, and consequently, retarded the catalyst deactivation. The reactive carbonate species formed on the magnesium oxide in the Ni-Mg/HY catalyst played an important role in suppressing carbon deposition on the catalyst surface.

Keywords: Methane reforming with carbon dioxide; Ni/HY catalyst; Synthesis gas; Promoter; Carbon deposition

1. Introduction

The catalytic reforming of methane with carbon dioxide (dry reforming) to synthesis gas ($CO_2 + CH_4 \rightarrow 2CO + 2H_2$) has attracted much attention, because it can produce synthesis gas having a low H_2/CO ratio (1:1) that is desirable for direct use as a feedstock for the production of oxygenated derivatives. This reaction is also of great importance in an environmental point of view, because methane and carbon dioxide, well-known greenhouse gases, can be converted into a valuable feedstock [1–3].

Numerous supported catalysts such as nickel- and novel metal-based catalysts have been investigated for the methane reforming with carbon dioxide. These examples include Ni/La_2O_3 [4], Ni-YSZ-CeO_2 [5], Ni/MnO-Al_2O_3 [6], Co/MgO [7], Pt/Al_2O_3 [8], Ni/ZrO_2 [9], Ni/CeO_2-Al_2O_3 [10], Pt/ZrO_2 [11], Rh/SiO_2 [12], Ni/CaO-Al_2O_3 [13], Ni/SrO-Al_2O_3 [14], $La_{2-x}Sr_xNiO_4$ [15], and Ni/Al_2O_3 [16–20] catalysts. One of the serious problems in the methane reforming with carbon dioxide is the carbon deposition formed via the Boudouard reaction ($2CO \rightarrow C + CO_2$) or methane decomposition ($CH_4 \rightarrow C + 2H_2$), which eventually leads to catalyst deactivation, plugging of the reactor, and breakdown of the catalyst [21–28]. It is well known that noble metal catalysts are less sensitive to carbon deposition compared to nickel-based catalyst. But the high market price of noble metals renders their industrial application quite questionable. Therefore, it is more practical from an industrial standpoint to develop an improved non-novel metal-based catalyst. It is necessary to develop supported catalysts comprising nickel and promoter, which show considerable catalytic activity without experiencing catalyst deactivation by carbon deposition.

The addition of small amounts of steam in the methane reforming with carbon dioxide has been investigated in order to prevent carbon deposition on the supported nickel catalysts. However, more promising method for preventing carbon deposition, and thus, for improving catalytic performance and stability is to modify the supported nickel catalysts by promoters. Typical modification of nickel-based catalysts has been done with alkali or alkaline earth metal oxides, and group VII or VIII transition metal oxides, as listed above [6,10,13,14].

Reported in this work are characterization, catalytic activity, and stability of Ni/HY catalysts modified by Mg, Mn, K, and Ca promoters in the methane reforming with carbon dioxide.

* Corresponding author. Tel.: +82 2 880 9227; fax: +82 2 888 7295.
E-mail address: inksong@snu.ac.kr (I.K. Song).

1381-1169/$ – see front matter © 2005 Elsevier B.V. All rights reserved.
doi:10.1016/j.molcata.2005.10.013

The effect of promoter on the performance of Ni/HY catalyst was investigated in detail, with an aim of minimizing carbon deposition on the catalyst surface and improving stability of the catalyst.

2. Experimental

2.1. Catalyst preparation

A series of Ni/HY catalysts promoted by Mg, Mn, K, and Ca were prepared by co-impregnation method with an aqueous solution containing nickel nitrate ($Ni(NO_3)_2 \cdot 6H_2O$) and promoting metal nitrate. In short, nickel nitrate and promoting metal nitrate with desired mole ratio were dissolved in distilled water, and the solution was then mixed with HY zeolite support in a rotary vacuum evaporator at 60 °C, followed by evaporation of water. The impregnated catalysts were dried overnight at 100 °C, and then they were calcined in a helium flow at 400 °C for 3 h. Prior to the catalytic reaction, the prepared catalysts were reduced with a mixed a stream of hydrogen (10%) and nitrogen (90%) at 500 °C for 3 h.

2.2. Catalytic reaction

Methane reforming with carbon dioxide was carried out in a continuous flow fixed-bed reactor at an atmospheric pressure. Fig. 1 shows the schematic diagram of reaction set-up. A quartz tube (inner diameter = 8 mm and length = 300 mm) was used as a reactor. The reactor was placed inside an electric furnace equipped with a PID temperature controller. A thermocouple connected to the temperature controller was placed on the top of the catalyst bed in order to monitor and control the reaction temperature. All catalytic reactions were conducted at 700 °C. Reactant gas stream comprising methane and carbon dioxide with a mole ratio of 1:1 was introduced into the reactor at a total feed flow rate of 200 ml/min diluted with nitrogen carrier gas for 1 g of each catalyst. The reaction products were periodically sampled and analyzed with an on-line gas chromatography (HP 6890) equipped with a thermal conductivity detector.

2.3. Catalyst characterization

Crystal states of the catalysts were investigated by XRD measurements (Rigaku, D/MAX-2000), and the sizes of nickel species were determined using Scherrer equation. Specific surface area, pore size, and pore volume of the catalysts were obtained using BET apparatus (Micromeritics, ASAP 2010). For infrared spectroscopy measurements, the catalyst powder was pressed into a self-supporting wafer, and it was analyzed using FT-IR spectrometer (Perkin-Elmer 1800 spectrometer). The amounts of carbon formed on the catalysts were determined by TGA measurements (TA instruments, SDT2690), which were carried out in an oxygen-containing atmosphere.

3. Results and discussion

3.1. Effect of Ni loading on the performance of Ni/HY catalyst

Effect of nickel loading on the performance of Ni/HY catalyst in the methane reforming with carbon dioxide is summarized in Table 1. Conversions and product yields were increased with

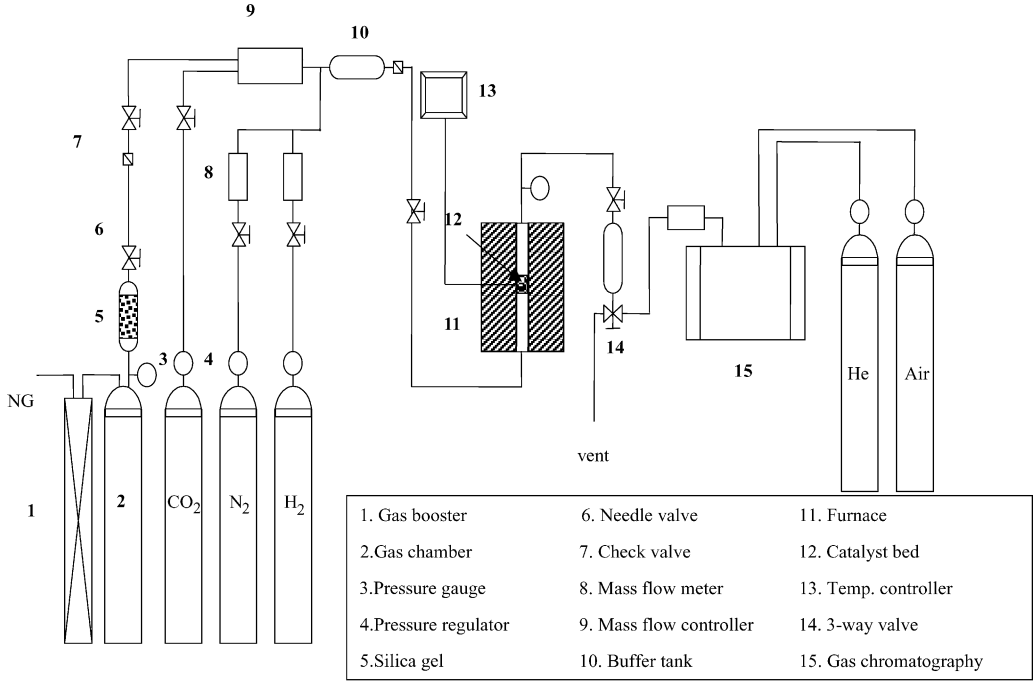

Fig. 1. Schematic diagram of reaction set-up for the methane reforming with carbon dioxide.

Table 1
Effect of Ni loading on the performance of Ni/HY catalyst in the methane reforming with carbon dioxide at 700 °C after 1 h reaction

Ni loading (wt.%)	Conversion (%)		Yield (%)	
	CH_4	CO_2	H_2	CO
5	35	39	32	45
10	84	74	66	69
13	93	86	82	87
20	78	72	76	77

increasing nickel loading up to 13 wt.%. At higher nickel loading more than 13 wt.%, the catalytic performance of Ni/HY catalyst started to decrease. It is believed that large nickel species on the surface of 20 wt.% Ni/HY catalyst led to carbon deposition over active metal species, which eventually caused the catalyst deactivation. The 13 wt.% Ni/HY catalyst exhibited 93% methane conversion and 82% hydrogen yield after 1 h reaction at 700 °C.

3.2. Effect of promoter on the catalytic activity and stability of Ni/HY catalyst

Effect of promoter on the performance of Ni/HY catalyst in the methane reforming with carbon dioxide at 700 °C is shown in Fig. 2. Nickel and promoter contents were fixed at 13 and 5 wt.%, respectively. Initial activities over Ni/HY and metal-promoted Ni/HY catalysts were almost the same. After a certain period of catalytic reaction, however, it was revealed that Mg, Mn, and Ca promoters improved the catalytic performance without experiencing severe catalyst deactivation. The catalytic performance was decreased in the order of Ni-Mg/HY > Ni-Mn/HY > Ni-Ca/HY > Ni/HY > Ni-K/HY. It is noticeable that the addition of Mg to the Ni/HY catalyst remarkably stabilized the catalytic performance and retarded the catalyst deactivation. The Ni-Mg/HY catalyst showed methane conversions more than ca. 85%, without significant catalyst deactivation even after the 72 h catalytic reaction. The stability index, defined as the ratio of methane conversion at 72 h with respect to that at 1 h was 0.96 in the Ni-Mg/HY catalyst. Furthermore, average H_2/CO mole ratio in the product stream over the Ni-Mg/HY catalyst during 72 h reaction

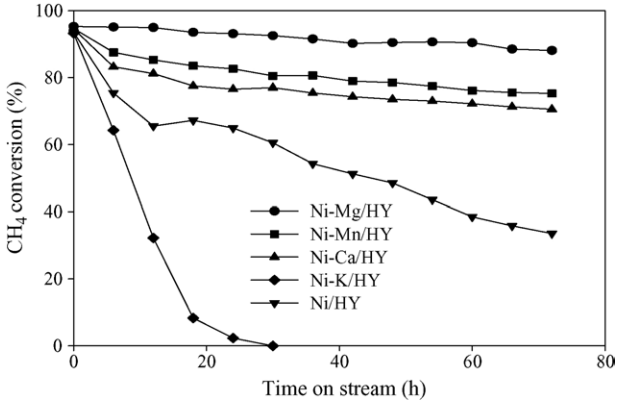

Fig. 2. Effect of promoter on the performance of Ni/HY catalyst in the methane reforming with carbon dioxide at 700 °C (GHSV = 3500 h^{-1}).

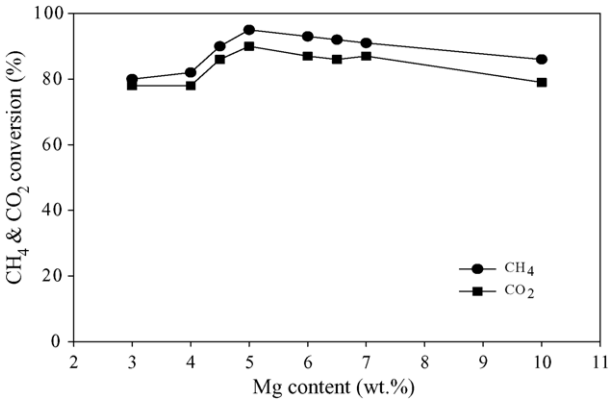

Fig. 3. Effect of Mg loading on the performance of Ni/HY catalyst in the methane reforming with carbon dioxide at 700 °C after 1 h reaction (Ni loading = 13 wt.%).

was 0.97 (≈1.0). On the other hand, the Ni-K/HY catalyst experienced severe catalyst deactivation, because reactor plugging occurred due to the formation of large amounts of coke even after 24 h reaction.

The primary effect of promoter addition to the Ni/HY catalyst in the methane reforming with carbon dioxide is to retard catalyst deactivation by suppressing carbon deposition on the catalyst surface [29]. It is believed that patches of partially reduced metal oxide species such as MgO_x and MnO_x cover a part of the nickel surface [30]. Such a decoration of nickel by metal oxide controls the nickel ensemble size on the HY zeolite surface [31]. Fine nickel species prohibit the formation of carbon deposition and enhance the catalytic performance in the methane reforming with carbon dioxide.

The carbon deposition in the methane reforming with carbon dioxide may occur via extensive methane decomposition and/or CO disproportionation. These two processes are believed to take place favorably on the large nickel ensembles. However, it was claimed that basic oxides increased the electron density of nickel, and thus, reduced the ability of nickel for extensive methane decomposition [24].

3.3. Effect of Mg loading on the performance and stability of Ni/HY catalyst

Fig. 3 shows the effect of Mg loading on the performance of Ni/HY catalyst in the methane reforming with carbon dioxide at 700 °C after 1 h reaction. The catalytic performance was remarkably increased with increasing Mg loading up to 5 wt.%. At higher Mg loading more than 5 wt.%, however, the catalytic performance of Ni-Mg/HY catalyst was slowly decreased. The Ni-Mg/HY catalyst containing 5 wt.% Mg promoter exhibited 93% methane conversion and 89% hydrogen yield after 1 h catalytic reaction.

The stability of Ni-Mg/HY catalyst containing 5 wt.% Mg promoter was examined by conducting the methane reforming with carbon dioxide at 700 °C for 720 h, as shown in Fig. 4. Only a slight catalyst deactivation was observed in the Ni-Mg/HY catalyst even after 720 h catalytic reaction. The amounts of carbon accumulated on the Ni-Mg/HY catalyst

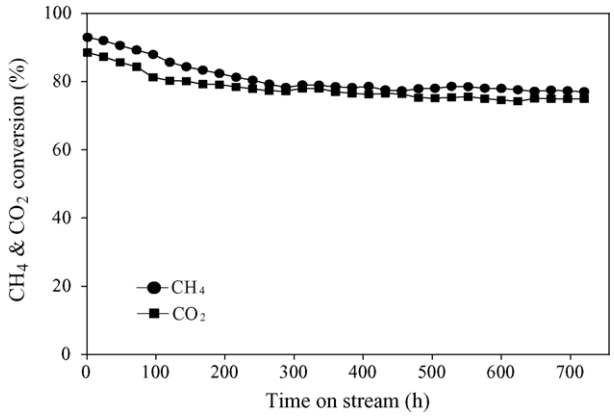

Fig. 4. Stability of Ni-Mg/HY catalyst containing 5 wt.% Mg promoter in the methane reforming with carbon dioxide at 700 °C for 720 h (CH_4/CO_2 = 1.0 and GHSV = 3500 h^{-1}).

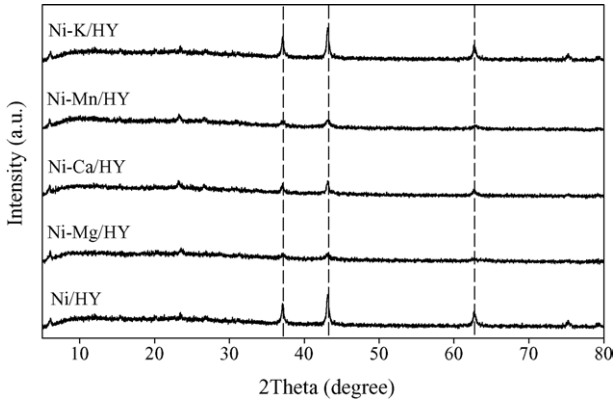

Fig. 5. XRD patterns of freshly calcined catalysts.

after 720 h catalytic reaction, which was determined by the weight loss of Ni-Mg/HY catalyst using TGA, were found to be 21 wt.%. In spite of the large amounts of carbon deposited on the catalyst surface, no significant loss of catalytic performance was observed in the Ni-Mg/HY catalyst, indicating that some part of carbon species did not act as a poison. It is also noticeable that methane conversion was similar to carbon dioxide conversion with time on stream, implying that the addition of Mg promoter suppressed the reverse water–gas shift reaction.

3.4. Physicochemical property and XRD analysis

Physicochemical properties of the prepared catalysts are summarized in Table 2. It was observed that pore diameter of Ni/HY catalyst was drastically decreased upon addition of promoter. The Ni/HY catalyst containing Mg promoter showed higher surface area and larger pore volume than any other catalysts. This result implies that the density of mesopores in the Ni-Mg/HY catalyst was higher than that in the other catalysts. The sizes of Ni species in both reduced and used catalysts were decreased with increasing surface areas.

Fig. 5 shows the XRD patterns of freshly calcined catalysts. In the Ni/HY and Ni-K/HY catalysts, NiO crystalline phases were clearly observed at 2θ = 37.2, 43.2, and 62.8°. Addition of Mg promoter drastically decreased the intensity of crystalline NiO peaks. This indicates that small NiO particles were formed in the Ni-Mg/HY catalyst, leading to strong interaction between NiO and MgO. The sizes of Ni species in the reduced and used catalysts determined from X-ray line broadening of Ni peak (2θ = 44.3°) were the smallest in the Ni-Mg/HY catalyst (Table 2), indicating that Ni species were highly dispersed on the surface of reduced Ni-Mg/HY catalyst. These results demonstrate that the addition of Mg promoter reduced the size of Ni species and produced the highly dispersed Ni species, and consequently, retarded the sintering of Ni species on the catalyst surface in the Ni-Mg/HY catalyst.

3.5. Carbon deposition on the Ni/HY and Ni-Mg/HY catalysts

The catalyst deactivation in this reaction is basically related to the deposition of inactive carbon species on the active metal sites. The amounts of carbon formed on the Ni-Mg/HY and Ni/HY catalysts after 72 h reaction were determined by TGA measurements, which were carried out in an oxygen-containing atmosphere (Fig. 6). TGA results showed that the weight losses of Ni/HY and Ni-Mg/HY catalysts were ca. 32 and 18%, respectively, indicating the formation of large amounts of carbon on the Ni/HY catalyst. The catalytic reaction was also conducted over the Ni-Mg/HY catalyst at 700 °C with a feed stream of $N_2/CH_4/CO_2$ = 5/3/1 in order to accelerate the catalyst deactivation by methane decomposition. Under such an unfavorable condition, however, the deactivation rate was only 0.52% per hour, although the amounts of carbon

Table 2
Physicochemical properties of the prepared catalysts

Catalysts	S_{BET} (BET surface area, m^2/g)	D_p (pore diameter, nm)	D_{micro} (micropore diameter, nm)	V_p (pore volume, cm^3/g)	D_{Ni}-reduced (diameter of Ni species, nm)	D_{Ni}-used (diameter of Ni species, nm)
Ni/HY	280.7	19.8	0.61	0.299	23.7	49.6
Ni-Mg/HY	352.7	4.3	0.43	0.428	14.9	18.8
Ni-Mn/HY	339.5	4.4	0.47	0.345	16.2	25.9
Ni-Ca/HY	298.4	4.1	0.45	0.365	19.5	30.1
Ni-K/HY	200.2	3.7	0.48	0.341	30.8	71.7

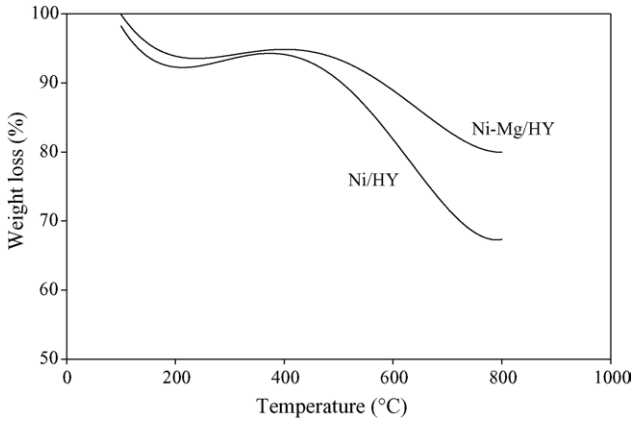

Fig. 6. TGA profiles of Ni-Mg/HY and Ni/HY catalysts after reaction at 700 °C for 72 h.

were increased (the weight loss determined by TGA was 21%).

3.6. Carbonate species on the Ni/HY and Ni-Mg/HY catalysts

Fig. 7 shows the IR spectra of Ni-Mg/HY and Ni/HY catalysts obtained after reaction at 700 °C for 72 h. It was observed that carbonate species appearing at ca. 1650 cm^{-1} were formed on the Ni/HY catalyst [32]. On the other hand, the Ni-Mg/HY catalyst showed a strong band at ca. 1550 cm^{-1}; the IR band at 1550 cm^{-1} can be assigned to carbonate species on magnesium oxide [33]. The nature of carbonate species between the two catalysts was totally different. Compared to carbonate species on the Ni/HY catalyst, carbonate species on the magnesium oxide was more reactive. It was previously reported that magnesium oxide with moderate basicity formed reactive surface carbonate species, which reacted with carbon deposited on the support by the methane decomposition [34]. Upon addition of Mg to the Ni/HY catalyst, reactive carbonate was formed on the magnesium oxide, and carbon dioxide could be activated more easily on the Ni-Mg/HY catalyst. Reactive carbonate species played an important role in inhibiting the carbon deposition on the catalyst surface.

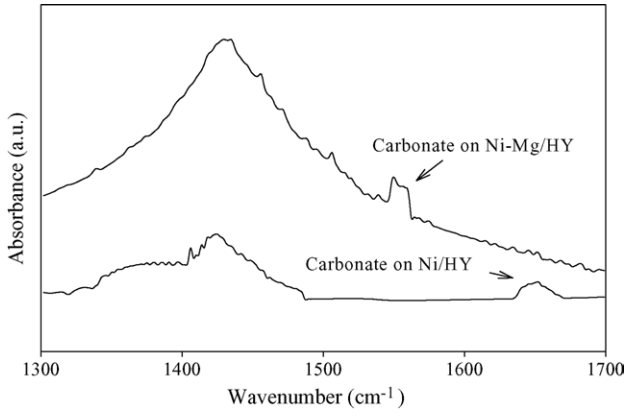

Fig. 7. FT-IR spectra of Ni-Mg/HY and Ni/HY catalysts after reaction at 700 °C for 72 h.

4. Conclusions

Methane reforming with carbon dioxide to synthesis gas was investigated over a series of Ni/HY catalysts promoted by Mg, Mn, K, and Ca. Among the catalysts tested in this work, the Ni-Mg/HY catalyst showed the highest carbon resistance and the most stable catalytic performance. Moreover, no significant loss of catalytic performance was observed in the Ni-Mg/HY catalyst during the reaction test period of 720 h. BET and XRD analyses revealed that the addition of Mg promoter reduced the size of Ni species and produced the highly dispersed Ni species, and consequently, retarded the sintering of nickel species on the catalyst surface in the Ni-Mg/HY catalyst. FT-IR results demonstrated that the reactive carbonate species formed on the magnesium oxide played an important role in suppressing carbon deposition on the catalyst surface.

References

[1] Z. Cheng, Q. Wu, J. Li, Q. Zhu, Catal. Today 30 (1996) 147.
[2] H.S. Potdar, H.-S. Roh, K.-W. Jun, M. Ji, Z.-W. Liu, Catal. Lett. 84 (2002) 95.
[3] S.-H. Seok, S.H. Choi, E.D. Park, S.H. Han, J.S. Lee, J. Catal. 209 (2003) 6.
[4] Z. Zhang, X.E. Verykios, Appl. Catal. A 138 (1996) 109.
[5] T. Kim, S. Moon, S.-I. Hong, Appl. Catal. A 224 (2002) 111.
[6] S.-H. Seok, S.H. Han, J.S. Lee, Appl. Catal. A 215 (2001) 31.
[7] H.Y. Wang, E. Ruckemstein, Appl. Catal. A 209 (2001) 207.
[8] K. Nagoaka, K. Seshan, K. Aika, J.A. Lercher, J. Catal. 197 (2001) 34.
[9] J.-M. Wei, B.-Q. Xu, J.-L. Li, Z.-X. Cheng, Q.-M. Zhu, Appl. Catal. A 196 (2000) L167.
[10] S. Wang, G.Q. Lu, Appl. Catal. B 19 (1998) 267.
[11] A.M. O'Connor, J.R.H. Ross, Catal. Today 46 (1998) 203.
[12] H.Y. Wang, C.T. Au, Appl. Catal. A 155 (1997) 239.
[13] A.L. Lemonidou, I.A. Vasalos, Appl. Catal. A 228 (2002) 227.
[14] Q. Jing, H. Lou, J. Fei, Z. Hou, X. Zheng, Int. J. Hydrogen Energy 29 (2004) 1245.
[15] J. Rynkowski, P. Samulkiewicz, A.K. Ladavos, P.J. Pomonis, Appl. Catal. A 263 (2004) 1.
[16] D. Halliche, R. Bouarab, O. Cherifi, M.M. Bettahar, Catal. Today 29 (1996) 373.
[17] S. Wang, G.Q. Lu, Appl. Catal. A 169 (1998) 271.
[18] J.-H. Kim, D.J. Suh, T.-J. Park, K.-L. Kim, Appl. Catal. A 197 (2000) 191.
[19] Z.X. Cheng, X.G. Zhao, J.L. Li, Q.M. Zhu, Appl. Catal. A 205 (2001) 31.
[20] A. Nandini, K.K. Pant, S.C. Dhingra, Appl. Catal. A 290 (2005) 166.
[21] G. Xu, K. Shi, Y. Gao, H. Xu, Y. Wei, J. Mol. Catal. A 147 (1999) 47.
[22] Z.L. Zhang, V.A. Tsipouriari, A.M. Efstathiou, X.E. Verykios, J. Catal. 158 (1996) 51.
[23] R.N. Bhat, W.M.H. Sachtler, Appl. Catal. A 150 (1997) 279.
[24] T. Horiuchi, K. Samura, T. Fukui, Y. Kubo, T. Osaki, T. Mori, Appl. Catal. A 144 (1996) 111.
[25] R. Cid, P. Atanasova, R.L. Cordero, J.M. Palacios, L. Agudo, J. Catal. 182 (1999) 328.
[26] A.A. Lemonidou, I.A. Vasalos, Appl. Catal. A 228 (2002) 227.
[27] J.H. Bitter, K. Seshan, J.A. Lercher, J. Catal. 176 (1998) 93.
[28] A. Huang, G. Xia, J. Wang, S.L. Suib, Y. Hayashi, H. Matsumoto, J. Catal. 189 (2000) 349.

[29] Y.-G. Chen, K. Tomishige, K. Fujimoto, Appl. Catal. A 161 (1997) 11.
[30] M.C.J. Bradford, M.A. Vannice, Appl. Catal. A 142 (1996) 97.
[31] H.M. Swaan, C.C.H. Kroll, G.A. Martin, C. Mirodatos, Catal. Today 21 (1994) 571.
[32] Z.L. Zhang, X.E. Verykios, S.M. McDonald, S. Affrossman, J. Phys. Chem. 100 (1996) 744.
[33] M. Baldi, E. Finocchio, C. Pistarino, G. Busca, Appl. Catal. A 173 (1998) 61.
[34] O.V. Krylov, A.K. Mamedov, S.R. Mirzabekova, Catal. Today 42 (1998) 211.